

# PRACTICAL ASPECTS OF CALIBRATING NEAR-INFRARED INTERFEROMETER DATA: PREDICTING STELLAR ANGULAR SIZES

Gerard T. van Belle

Jet Propulsion Laboratory, California Institute of Technology, 4800 Oak Grove Dr., Pasadena, CA 91109  
gerard@huey.jpl.nasa.gov

## Abstract

Reliable prediction of stellar diameters, particularly angular diameters, is a useful and necessary tool for the increasing number of milliarcsecond resolution studies being increasingly carried out in the astronomical community. Specifically, the task of calibrating visibility amplitude information from astronomical interferometers often requires the ability to reliably estimate diameters and uncertainties associated with those diameters. The ad hoc approaches generally used throughout the literature are discussed in a statistically rigorous manner; the relatively new and accurate technique of predicting a  $m_V=0$  apparent angular size is presented for both giant and supergiant stars, and for more evolved sources. Application of these techniques towards the task of normalizing visibilities from interferometers is also discussed in detail.

## 1. Introduction

In the last 15 years, near-infrared interferometers have evolved from rudimentary prototypes to the first generation of facility instruments, from the first fringes at CERGA (Di Benedetto & Conti 1983) to the Earth-scanned fringes at IRMA (Benson *et al.* 1991) to the recent near-IR first fringes with NPOI (Dyck 1998a). Previous to the results from long-baseline interferometry, lunar occultations were utilized in measuring stellar angular sizes (Ridgway *et al.* 1977) and continue to provide a steady stream of diameters (Richichi *et al.* 1998), to which the size determination techniques presented herein are equally applicable.

In interpreting long baseline interferometer data, one is frequently interested in establishing the point-source response of the instrument. This response can be measured by observing ‘calibration sources’ with the interferometer - sources that are effectively unresolved or close to unresolved by the interferometer, and reliably predicted as such. For ground-based installations, the calibrator response will be convolved with that of the atmosphere. Due to the temporal and spatial variations in response of the atmosphere, calibration sources are desired to be close to the science target(s) in both angle and in time. In this sense, calibration sources are utilized much like standard stars are for photometry. Use of calibration sources is well established in the infrared (cf. Di Benedetto 1985, Dyck *et al.* 1996) and the visible (cf. Mozurkewich *et al.* 1991, Baldwin *et al.* 1996). A detailed investigation of stellar surface brightness as a function of V-K color has already been published by Di Benedetto (1993), a study that is of course closely related to this questions of angular size being addressed by this manuscript.

One of the powerful aspects of interferometric data is the ability to provide precise angular sizes for large stars, even in the presence of large uncertainties for the smaller calibration sources. However, as astronomical interferometers have grown in size (from the 4.8 m baseline of IRMA to the 110m baseline of PTI; cf. Benson *et al.* 1991, Colavita *et al.* 1999), ‘unresolved’ sources have

become more scarce. The next generation of instruments (e.g. CHARA, Keck, VLTI; McAlister *et al.* 1994, Colavita *et al.* 1998, Mariotti *et al.* 1998) will have even larger baselines; offsetting this complication for the next-generation of instruments are larger apertures (typically 1 to 2 m, versus 12-40 cm) and improved detectors, allowing for use of more distant stars as calibration sources. However, for those more distant stars, only limited information is available - spectral typing, photometry, and parallaxes are all less available and less accurate. Deriving expected angular sizes - and determining the degree to which a given source is ‘unresolved’ or not - is a greater challenge in the face of these limitations. These limitations have already been eased somewhat with the release of the wealth of information represented by the Hipparcos catalog (Perryman *et al.* 1997) and will further be eroded with the future release of the data from the 2MASS and DENIS surveys that have limiting magnitudes of  $m_K > 14.3$  and 13.5, respectively (Beichman *et al.* 1998, Epchtein 1997).

## 2. Selection of Unresolved Calibration Stars

At the heart of selection of unresolved sources is establishment of a criterion for ‘unresolved’. Clearly such a criterion varies with baseline - a source unresolved for a 21m baseline might be well resolved at a facility with a 110m baseline. A given source will be adequate as a unresolved point-source reference based upon its expected size, and the uncertainty in that expected size. Simply put, a source qualifies as ‘unresolved’ if it cannot be discerned from a point source by a given instrument. The systematic limitations of an instrument’s response generally will establish what sources are truly unresolved. For example, for observing programs with typical seeing and well-selected calibrators (see §4), PTI has a night-to-night repeatability of  $\Delta V^2=0.018$  (van Belle *et al.* 1999). Within this limiting systematic error, PTI will be unable to distinguish sources with  $V^2 = 1.000$  and  $V^2 = 0.982$ . As we shall see below, this corresponds to stars with  $q \leq 0.36$  mas.

Sources that meet the criterion of establishing the zero-point of the instrument, but contribute to the zero-point

error at a level up but not exceeding to the systematic error due to uncertainties in their angular size estimates are also used quite commonly and shall be referred to as ‘partially resolved’ calibrators. Furthermore, sources that are even larger than this and are fully resolved by the instrument can be used to establish the zero point of the instrument, albeit at a lower degree of accuracy. These sources can be resolved stars whose angular sizes have been measured in the past, although care must be taken in using measurements at different wavelengths.

### 2.1 Uniform disk visibility

The visibility squared of a uniform disk is given as

$$V(x)^2 = \left( \frac{2J_1(x)}{x} \right)^2$$

where  $x = \pi q B / I_0$ , and  $J_1(x)$  is the first order Bessel function. Given an interferometer baseline  $B$ , wavelength  $I_0$  and stellar angular size  $q$ , an expected  $V^2$  can be determined; or conversely, a measured  $V^2$  and telescope parameters can deliver a uniform disk angular size. Stars are of course not uniform disks, but rather, limb-darkened or limb-brightened disks. These effects and their degree are wavelength-dependent. Fortunately, at  $2.2 \mu\text{m}$ , the effect of limb-darkening is quite small; modelling of these effects indicates it to be a  $\sim 2\%$  effect for giant stars (cf. Scholz & Takeda 1987, Dyck *et al.* 1996a), and these models are supported by observational evidence (cf. Tuthill 1994, Dyck *et al.* 1998b). At shorter wavelengths and for more evolved stars (carbon stars, Mira variables), the effects become more pronounced (cf. Scholz & Takeda 1987, van Belle *et al.* 1997) and need to be carefully considered.

### 2.2 Example of Unresolved Source Selection

From the limiting night-to-night repeatability for PTI of  $DV^2_N = 0.018$  (van Belle *et al.* 1999), it is possible to match the zero-point uncertainty to this limiting  $DV^2$ . Assuming that for any given star we can know its angular size to a relative error of 17% (see §3.3), a 0.60 mas star will have an uncertainty of 0.102 mas with an expected  $V^2$  of 0.949 with  $DV^2 = 0.018$ . Actually observing this source might result in a measured  $V^2$  of  $0.80 \pm 0.04$ , typical for a single observing set at PTI in nominal observing seeing conditions. The resultant normalization factor would be  $1.16 \pm 0.06$  for that set. Multiple observations of a given calibrator/target set can reduce the statistical uncertainty to the systematic limit set by the night-to-night repeatability and the calibrator angular size uncertainty. Given the  $DV^2 = 0.018$  uncertainty limitation, Table 1 lists estimated angular sizes and their associated acceptable error bars.

### 3. Estimation of Stellar Angular Sizes

Given that a desired expected angular size and its associated uncertainty level have been established, the next step is to derive those angular sizes. A number of tools are at our disposal. First, linear radius can be used in conjunction with distance to estimate angular size. Second, under the assumption of black body behavior, wide-band

photometry fitted to a Planck function can also deliver angular sizes. Third, use of existing angular sizes can be used to establish a relationship between V-K color and  $V=0$  apparent angular sizes.

#### 3.1.1 References in the Literature

As a test of the methods discussed, we shall be examining the predictions of the various estimators against known angular diameters. For stars that have evolved off of the main sequence, angular diameters as determined in the near-infrared are preferred, as the effects of limb darkening – and the need for models to compensate for them – are less than at shorter wavelengths. There are four primary sources in the literature of near-infrared angular diameters (primarily K band):

*Kitt Peak*. The lunar occultation papers by Ridgway and his coworkers (Ridgway *et al.* 1977a, 1977b, 1979, 1980a, 1980b, 1982a, 1982b, 1982c, Schmidtke *et al.* 1986) established the field of measuring angular sizes of cool stars in the near-infrared. This effort is no longer currently active.

*TIRGO*. The lunar occultation papers by Richichi and his coworkers (Richichi *et al.* 1988, 1991, 1992a, 1992b, 1995, 1998a, 1998b, 1998c, 1998d, Di Giacomo *et al.* 1991) have continued and further developed this particular technique of diameter determinations. The group is continuing to vigorously explore the high-resolution data obtainable from lunar occultations. The recent publications from the TIRGO group include data from medium to large aperture telescopes (1.23m – 3.5m), along with concurrent photometry.

*IOTA*. The five K band angular diameters papers from the Infrared-Optical Telescope Array by Dyck and his coworkers (Dyck *et al.* 1996a, 1996b, 1998b, van Belle *et al.* 1996, 1997) provided a wealth of information on normal giant and supergiant papers, and also on more evolved sources such as carbon stars and Mira variables. Recently, results from this interferometer from the FLUOR experiment have also become available (Perrin *et al.* 1998).

*PTI*. Although there is only one angular diameter paper currently available from PTI (van Belle *et al.* 1999),

Estimated Angular Size (mas)	Expected $V^2$
0.100 +- 0.271	0.999 +- 0.018
0.200 +- 0.210	0.994 +- 0.018
0.300 +- 0.168	0.987 +- 0.018
0.400 +- 0.138	0.977 +- 0.018
0.500 +- 0.117	0.964 +- 0.018
0.600 +- 0.102	0.949 +- 0.018
0.700 +- 0.091	0.931 +- 0.018
0.800 +- 0.082	0.911 +- 0.018

Table 1. Allowable errors in angular size, based upon matching a night-to-night limiting  $DV^2 = 0.018$  residual error with  $B = 110\text{m}$ ,  $\lambda = 2.2\mu\text{m}$ .

69 objects are presented in the manuscript from this highly automated instrument.

In addition to these near-infrared observations, shorter wavelength observations were used to obtain diameters for main sequence objects – few near infrared observations exist for these smaller sources. These objects were culled from the catalog by Fracassini (1988), limiting the investigation to direct angular size measures found in that catalog: lunar occultations, eclipsing and spectroscopic binaries, and the intensity interferometer observations of Hanbury Brown *et al.* (1974). Unfortunately, the sample of main sequence objects is much smaller than for giant stars, largely reflecting the current resolution limits (roughly 1 mas) in both the interferometric and lunar occultation approaches.

### 3.1.2 Error Bars and Confidence Levels

One particularly important point to note is the concept of error bars and confidence levels. The norm in the literature discussed above is to quote  $1\sigma$  error bars. It is equivalent to state that these error bars correspond to a single standard deviation of the data, or, under the assumption of a Gaussian distribution, that these error bars correspond to the 68% confidence level. The two and three sigma error bars correspond to the 95% and 99% confidence level, respectively.

In the interest of establishing calibration sources, one is interested in determining *a priori* that one or more sources will be unresolved. In practice, it is often the case that multiple calibrators are initially used in an observing run, until one of the potential calibration objects has been observationally verified as actually having a visibility indistinguishable from a point source. If the predicted size for a supposed point source has only a  $1\sigma$  error bar associated with it, then there is a 32% chance that the actual size will fall outside of the expected range, and as such, there is a substantial chance that the source could be unsuitable for use as a calibrator.

Under the assumption that out of multiple calibrators, a single good calibrator can be used to disqualify the other poor calibrators, a potential approach is to utilize numerous sources with less confidence associated with their size (1 or  $2\sigma$  errors). Less calibrators with more confidence is also valid, assuming that such objects are to be found. In Table 2, the confidence levels associated with 1, 2, and 3s error bars is listed, along with the probability  $P$  of not finding a single suitable calibrator when multiple stars are used for each confidence level. Taking 0.3% as a reasonable upper limit to the acceptable probability that the selected

s	Confidence Level	P		
		1 star	2 stars	3 stars
1	0.68	0.32	0.10	0.03
2	0.95	0.05	0.003	0.0001
3	0.99	0.01	0.0001	1.0E-06

Table 2. Probability P of 1, 2, or 3 stars falling with expected size range, based upon 1, 2, or 3s error bars.

calibrators are not the size expected, we see that 2 or more calibrators with at least a  $2\sigma$  error associated with their size is appropriate. This corresponds to the loss of one observation set in 300 due to improper calibration.

### 3.2 Linear Radius

Based upon the distance to a star and its expected linear radius, an angular size can be derived. Simply put, the relationships between angular diameter  $q$  (mas), linear radius  $R$  ( $R_{SUN}$ ), parallax  $p$  (mas), and distance  $d$  (pc) are:

$$\begin{aligned} q &= 2 \times R \times 6.96 \times 10^8 \frac{\text{m}}{R_{SUN}} \times \frac{1}{d \times 3.09 \times 10^{16} \frac{\text{m}}{\text{pc}}} \times 206265000 \frac{\text{milliarcsec}}{\text{radian}} \\ &= 9.292 \times \frac{R}{d} \\ &= 2 \times R \times 6.96 \times 10^8 \frac{\text{m}}{R_{SUN}} \times \frac{1}{\frac{1}{p} \times 1000 \times 3.09 \times 10^{16} \frac{\text{m}}{\text{pc}}} \times 206265000 \frac{\text{milliarcsec}}{\text{radian}} \\ &= 0.009292 \times R p \end{aligned}$$

The obvious caveat is that the conventions are for linear *radius* and angular *diameter* - going from linear radii to angular diameters often have an overlooked factor of 2. The mathematics involved in this approach is the most straightforward - assuming one can provide realistic values for  $R$  and  $d$  (or  $p$ ), and their uncertainties.

#### 3.2.1 Data Sources for Linear Radius Method

*Distance.* The primary sources for stellar distances is the Hipparcos catalog (Perryman *et al.* 1997). Its collection of parallaxes for 118,000 stars out to 1 kpc is impressive and extraordinarily useful, particularly for this application. However, for limiting the impact of the catalog's  $\sim 1$  mas errors, it is prudent to limit use of parallaxes to those that indicate distances of 300 pc or less.

*Linear Radius by Spectral Type: Main Sequence Stars.* Using the main sequence star sample as noted above, a mean radius-spectral type relationship is found for these objects:

$$R = 1.21 \pm 0.22 + 1.47 \pm 0.38 \times 10^6 \times \text{SP}^{-4.17 \pm 0.07} R_{SUN},$$

for B0 (SP=20) through G3 (SP=53). Size predictions had 1, 2, and 3s errors corresponding to 25%, 42% and 60%, respectively. The size of this error bar is an indicator of two aspects of spectral typing in this application: first, it is often not accurately or consistently done (particularly with regards to determination of luminosity class along with spectral type), and second, it is not particularly adequate as a single parameterization for deriving radius.

*Linear Radius by Spectral Type: Giant Stars.* From van Belle *et al.* (1999), the empirical relationship based upon 95 luminosity class III stars is:

$$R = 4.04 \pm 1.40 + 9.58 \pm 0.84 \times 10^{(0.096 \pm 0.006 \times (\text{SP}-60))} R_{SUN},$$

where SP=57, ..., 65, 66, ..., 72 for spectral types G7, ..., K5, M0, ..., M6. For the fit, the average absolute

deviation was 22%; the  $2\sigma$  error bar is 37% and the  $3\sigma$  error bar is 52% of a given value for R.

*Linear Radius by V-K Color: Main Sequence Stars.* No clear correlation seen between V-K color and main sequence star linear diameters. This is consistent with both bandpasses being on the Rayleigh-Jeans tail of the Planck function for most of these hot ( $T > 5000\text{K}$ ) stars.

*Linear Radius by V-K Color: Giant Stars.* As with the linear radius - spectral type relationship, also found in van Belle *et al.* is an empirical relationship for linear radius as a function of V-K color. For the range of V-K from 2.0 to 6.0, linear radius is given by:

$$R = 1.76 \pm 0.13 \times (V-K)^{2.36 \pm 0.06} R_{\text{SUN}};$$

the average absolute deviation over that range is 22%; the  $2\sigma$  error bar is 36% and the  $3\sigma$  error bar is 51% of a given value for R.

### 3.3 Bolometric Flux

Fitting a Planck curve to wide-band photometry can lead to an estimate of temperature and angular size. Considerable photometry exists for many stars from U to K (and longward) which can be readily accessed over the Internet (see §3.2.2). Many (though certainly not all) stars are adequately characterized as black-body radiators for the purposes of this paper. On the low end of the temperature scale, stars down to 3500K do not depart from BBR behavior significantly. The high end of the temperature scale is determined by the available photometry and the desire to fit at least a portion of BBR curve that is departing significantly from Rayleigh-Jeans behavior. Also, since results on the hotter stars depend more heavily upon the short wavelengths, both adequate corrections for reddening and short wavelength atmospheric effects such as the Balmer discontinuity become much more important.

Although the actual computations obtaining an angular size estimate from photometric data is a little more challenging, the results tend to be a bit better than the linear radius method.

#### 3.3.1 BBR Fit Validity

*Main Sequence Stars.* Main sequence stars between B and G spectral types are ideal calibrators when UBVRJHK photometry is available. For example, an excellent main sequence calibrator is 51 Peg. A great deal of photometry between the visible and mid-IR is available, and it is nearby with a well-determined distance. In spite of its celebrated radial velocity variability, this object observed with an IR interferometer is merely a bright, unresolved calibrator with a steady  $V^2$  (Boden *et al.* 1998).

There were 39 main sequence stars with sufficient photometry to determine a blackbody fit and corresponding angular size  $q_{\text{BBR}}$ ; these objects were of spectral types B, A, F, and G. For the 20 with objects  $q_{\text{ACTUAL}} > 0.3$  mas, the corresponding relationship between blackbody diameters and measured diameters was fit as:

$$q_{\text{MEASURED}} = -0.005 \pm 0.175 + 0.999 \pm 0.147 \times q_{\text{BBR}}$$

which indicates a slight tendency  $q_{\text{BBR}}$  to overestimate the stellar angular size, but is statistically identical to a straight line. The 1, 2 and  $3\sigma$  relative error bars for this sample are 27%, 54% and 81%, respectively (regardless of whether or not the above line fit was used to de-trend the BBR angular sizes). For the whole sample, the fit was:

$$q_{\text{MEASURED}} = -0.093 \pm 0.165 + 1.042 \pm 0.171 \times q_{\text{BBR}}$$

where clearly the overestimation tendency of  $q_{\text{BBR}}$  is becoming statistically significant. The 1, 2 and  $3\sigma$  relative error bars for this sample are 41%, 81% and 121%, respectively, when the above fit is used to de-trend the data.

As suggested above, the reason for the stars with smaller angular extent being overestimated in size by a blackbody fit is most likely either insufficiently corrected interstellar extinction or short wavelength non-grey opacity effects. The smaller stars tend to be either hotter or more distant objects, or both. Although the fits noted above were adjusted for interstellar extinction based upon the Hipparcos parallax, if any residual reddening were present in the data, there would be a tendency for the blackbody fits to appear cooler and larger. Flux depressions of 5-10% in the 0.4-0.5  $\mu\text{m}$  bandpasses, with none in the  $\lambda > 1.0 \mu\text{m}$  bandpasses (corresponding roughly to the perceived effects of interstellar extinction) would make the blackbody fit for a 15,000K star appear to be 14,000K, with a  $\sim 10\%$  increase in size. Furthermore, the growing effect of the Balmer discontinuity for stars with  $T_{\text{EFF}} > 7,000\text{K}$  make the BBR approach highly questionable for the hotter stars.

*Giant and Supergiant Stars.* There is a general tendency for blackbody fits to overestimate the sizes of giant and supergiant stars. This tendency does not appear to be any more severe for luminosity class I and II stars versus giants, but does appear to become more aggravated as blackbody fits are performed on later and later spectral types. The parameters for the linear relationship between predicted size and actual measured size can be seen in Table 3. These parameters were determined for both photometrically well-sampled stars, and for stars with poor photometric coverage; the outcomes do not appear to vary greatly.

Also given in Table 3 is the ratio between blackbody fit diameters and measured diameters. As can be seen for the F and G class giant and supergiant subset, the departure from blackbody behavior is not statistically significant; for the K class objects, the departure is beginning to manifest itself but is only a  $\sim 15\%$  effect at the  $1\sigma$  level. For the M class objects, the effect is larger, but with a great deal of spread; the roughly  $\sim 60\%$  effect has a standard deviation of 40-60%, depending upon the sample cut.

Finally given in Table 3 are the 1, 2, and  $3\sigma$  relative errors associated with the various samples. These relative errors were obtained from angular sizes obtained from bolometric flux fits, and then adjusted according to the slope and intercepts given in the table. As a result of the adjustment, the average relative difference for all of the

objects in a given set is zero. Consistent with this discussion is the result that the F, G, and K type stars have relatively little spread when compared to the M type stars. Also apparent from the relative errors is the slight improvement in size prediction for those stars where large amounts of photometry exists.

### 3.3.2 Sources of Photometry on the Internet

*General Data.* One of the more thorough references on stellar objects is SIMBAD (<http://simbad.u-strasbg.fr/>, France, and <http://simbad.harvard.edu/>, US Mirror; note that registration is required for use). In addition to the web-based query forms, one may also obtain information from SIMBAD by telnet and email. It is important to note that SIMBAD is merely a clearing house of information from a wide variety of sources and is not an original source in and of itself; any information that ends up being crucial to the merit of an astrophysical investigation should be checked against its primary source.

*Infrared Photometry ( $I > 1\text{mm}$ ).* The Catalog of Infrared Observations, a extensive collection of IR photometry by Gezari *et al.* (1993) has been updated, although the most recent version is available only online (Gezari, Pitts & Schmitz 1997). The latter catalog can be queried with individual stars or lists of objects at VizieR (<http://vizier.u-strasbg.fr/>, US Mirror at <http://adc.gsfc.nasa.gov/viz-bin/VizieR>). As with the SIMBAD data, Gezari is merely a collection of the data in the literature, and examination of the primary sources is advised.

*Visual Photometry.* The General Catalog of Photometric Data (GCPD) provides a large variety of wide-to narrow-band visual photometry at <http://obswww.unige.ch/gcpd/gcpd.html>. For variable stars, the AAVSO and AFOEV are both excellent sources of epoch-specific V band photometry.

*Ultraviolet Photometry ( $I < 0.4\text{mm}$ ).* For the hotter stars ( $T > 7,000\text{ K}$ ), the peak of the blackbody curve is shortward of  $\lambda = 0.4\mu\text{m}$ . In the absence of short wavelength photometry, fitting a blackbody curve with strictly points on the Rayleigh-Jeans end of the blackbody curve can easily lead to improper fits – the peak of the curve is not well determined. In the presence of that photometry, the depression of the short wavelength points by the increasing H opacity can incorrectly indicate cooler, larger stars. As such, the hotter stars that require photometry shortward of the B band for a proper BBR fit will probably not be appropriate for application of that fit.

### 3.4 V=0 Apparent Angular Size versus V-K Color

The large body of available angular sizes allows for directly inferring expected angular sizes, bypassing considerations of stellar distance, spectral type, reddening, and linear size. To compare angular sizes of stars at different distances, one approach is to scale the sizes relative to a value of  $m_V=0$ :

$$q_{V=0} = q \times 10^{V/5},$$

or likewise with  $m_K=0$  (see Dyck *et al.* 1996). The angular size thus is scaled to a constant brightness distance and becomes a measure of apparent surface brightness. Conversion between a V=0 apparent angular size and actual apparent angular size is trivial with a known V magnitude and the equation above.

*Giant and Supergiant Stars.* By examining the 2.2  $\mu\text{m}$  angular sizes for the 164 normal giant and supergiant stars found in the interferometry and lunar occultation papers, we can establish a relationship between V=0 apparent angular size and V-K color:

$$q_{V=0} = 10^{0.682 \pm 0.014 + 0.222 \pm 0.003 * (V-K)}$$

The 1, 2, and 3s errors from the average absolute deviations of measured values from the fit correspond to 10%, 17% and 25%.

For the giant stars, the relationship appears valid over a V-K range of 2.0 to 8.0. Blueward of V-K=2.0, the subsample is too small (N=3) to confidently indicate whether or not the fit is valid, in spite of the goodness of fit for the whole subsample. The same is true redward of V-K=8.0. Also, for stars redward of approximately V-K = 8, care must be taken to not be evaluating variable stars (both semiregular and Miras). The data points and the fit noted above may be seen in Figure 2;  $q_{V=0}$  and standard deviation by V-K bin is given in Table 4.

The potential misclassification of more evolved sources such as carbon stars and variables (Miras or otherwise) as normal giant and supergiant stars is a significant secondary consideration. For the dimmer sources for which little data is available, non-classification is perhaps the more appropriate term. What is reassuring with regards to the issue of classification errors is the fact that the robust relationship between  $q_{V=0}$  and V-K is valid for stars of luminosity class I, II, and III. Our experience with the available data is that errors exist more frequently in luminosity classifications rather than in typing by chemical abundance or variability. However, since the  $q_{V=0}$  relationship is insensitive to errors in luminosity class, this method is more robust than the linear radius-distance method, particularly for those stars in the 2.0 < V-K < 5.0 range, where few if any stars of significant variability exist. This relationship is also easier to employ than the method of BBR fits.

*Evolved Sources: Variable Stars.* By examining the 2.2  $\mu\text{m}$  angular sizes for the 88 semiregular variables, Mira variables and carbon stars (broadly classified here as ‘variable stars’) found in the literature, we can establish a relationship between V=0 apparent angular size and V-K color:

Spectral Types	Luminosity Class	DOF	N	Slope b	Intercept a	Ratio	1σ	2σ	3σ
All	all	all	201	1.45	-0.68	1.45±0.53	0.182	0.350	0.517
FG	all	>15	9	1.27	-0.55	1.00±0.14	0.072	0.125	0.177
K	all	>15	30	1.32	-0.57	1.17±0.14	0.081	0.148	0.215
M	all	>15	46	1.60	-1.01	1.59±0.38	0.200	0.393	0.585
FG	all	all	14	1.16	-0.25	1.02±0.14	0.080	0.156	0.232
K	all	all	52	1.29	-0.38	1.15±0.30	0.095	0.174	0.252
M	all	all	132	1.75	-0.91	1.62±0.55	0.210	0.448	0.687
M	III	>15	35	1.81	-2.79	1.60±0.41	0.190	0.386	0.581
M	III	all	113	1.66	-1.02	1.62±0.57	0.232	0.521	0.809

Table 3. Linear relationship  $q_{\text{BBR}} = a + b \times q_{\text{ACTUAL}}$  between blackbody and actual angular sizes for luminosity class I, II and III oxygen-rich stars. *DOF* is the number of photometry data point degrees of freedom for the blackbody fits; *N* is the number of stars available for each subset. Ratio is the average value of  $q_{\text{BBR}} / q_{\text{ACTUAL}}$  for each subset. The error bars given are for the average relative difference between  $q_{\text{ACTUAL}}$  and  $q_{\text{BBR}}$ , when  $q_{\text{BBR}}$  has been adjusted based upon the linear parameters *a* and *b*; for these cases,  $q_{\text{BBR}} / q_{\text{ACTUAL}} = 1$  for each subset.

$$q_{V=0} = 10^{0.801 \pm 0.039 + 0.220 \pm 0.005 * (V-K)}$$

The fractional deviation of fit from measured angular sizes is 21%. Given a standard deviation of the absolute deviations of 17%, the 95% and 99% confidence levels correspond to 38% and 54% errors, respectively. The data points and the fit noted above may be seen in Figure 3.

For the variable stars, the relationship appears valid over a V-K range of 5.5 to 13.0. Redward of V-K=13, the sample is too small (N=3) to confidently indicate whether or not the fit is valid, in spite of the goodness of fit for the general sample. It is interesting to note that the slope of the fits for the variable stars and for the giant/supergiant stars is statistically identical; only the intercepts are different. This corresponds to a  $q_{V=0}$  difference of roughly 30% between ‘normal’ and ‘variable’ stars for a given V-K color.

*Main Sequence Stars.* By examining the objects in the Fracassini catalog (1988, specifically many objects from Hanbury Brown *et al.* 1974), there appears to be similar relationships between V-K color and V=0 angular size. However, the sample set of stars with adequate photometry is unfortunately limited, and drawing broad conclusions from the sample is potentially suspect. In the narrow range of  $-0.5 < V-K < +0.5$ , which is well sampled, the relationship between V-K and  $q_{V=0}$  is

$$q_{V=0} = 10^{0.503 \pm 0.027 + 0.328 \pm 0.166 * (V-K)}$$

The resulting average absolute difference between predicted and actual angular size is only 2%; the 2σ and 3σ ranges are 4% and 6%. These objects are plotted in Figure 4. Clearly, the relationship appears to not only hold for the B and A type objects in the  $0.5 < V-K < +0.5$  range, but also for the two G type stars seen at  $V-K \sim 1.5$ . Unfortunately, due to the limited sampling of the B, A, G type relationship, it is unclear how well the relationship noted in the equation above holds in the  $0.5 < V-K < 1.5$  range. For the cooler K and M type stars, at  $V-K > 1.5$ , the relationship clearly shifts just as with the normal giant/supergiants and the variables,

but towards a smaller, rather than larger apparent angular size. The intercept shifts from 0.503 to roughly 0.100, but there are again only a few (4) stars to support this observation.

### 3.5 Comparison of the Various Methods

Having looked in detail at the various tools available, and their associated uncertainties, it would be worthwhile to address the question of which method is preferred for establishing a calibration for an interferometer zero-point. The methods are summarized in Table 5. Clearly, of all the approaches, establishing a  $q_{V=0}$  angular size for main sequence stars delivers the best results (§3.3), but has only been established over a narrow range ( $-0.5 < V-K < +0.5$ ). The approaches of most general validity are  $q_{V=0}$  for giant and supergiant stars (§3.3), and angular size by blackbody fit for F, G, K giants and supergiants (§3.2). Following these approaches is blackbody fit for main sequence stars (§3.2).

### 4. Proximity Considerations

A vital concern in the selection of calibration sources for science targets is *proximity* - both spatial and temporal. Variability of both the atmosphere and instrument response with pointing and time can reduce or even eliminate the correlation between system performance for the calibration source and science target. The magnitude and nature of these effects are dependent upon both the particular interferometer, the general nature of the atmospheric performance at the site, and the specific behavior of the atmosphere for a given evening of observing. These concerns are unsurprising, given the parallels of photometry via the use of standard stars. Our experience with PTI indicates that calibration sources on typical observing nights may be no further than 15° and  $\pm 1^h$  from the science targets (Boden *et al.* 1998), and there is an improvement in response as the proximity is increased, most

V-K bin	Width	Normal giants and supergiants				Variables				Ratio
		N	Average $q_{V=0}$	Std. Dev.	Fit	N	Average $q_{V=0}$	Std. Dev.	Fit	
-0.5	0.5	1	3.4		3.7	0				
0.0	0.5	0			4.8	0				
0.5	0.5	0			6.2	0				
1.0	0.5	1	9.1		8.0	0				
1.5	0.5	2	11.6	1.8	10.3	0				
2.0	0.5	9	13.9	1.7	13.4	0				
2.5	0.5	17	16.7	3.1	17.2	0				
3.0	0.5	12	20.5	3.1	22.3	0				
3.5	0.5	20	27.2	4.4	28.7	0				
4.0	0.5	21	37.8	4.4	37.1	0				
4.5	0.5	16	47.5	6.0	47.9	0				
5.0	0.5	17	58.3	6.0	61.9	0				
5.5	0.5	15	80.3	13.9	79.9	4	105	13	103	0.25±0.05
6.0	0.5	7	102.7	13.3	103.1	7	140	25	132	0.31±0.07
6.5	0.5	5	122.9	18.3	133.1	9	181	57	170	0.36±0.13
7.0	0.5	9	159.6	23.5	171.9	8	233	60	220	0.32±0.09
7.5	0.5	6	197.0	21.0	222.0	14	270	62	283	0.28±0.07
8.0	0.5	0			286.6	9	461	184	365	
8.5	0.5	1	355.4		370.0	4	605	217	470	0.41±0.15
9.0	0.5	1	431.0		477.8	7	631	245	605	0.32±0.12
9.5	0.5					3	841	259	780	
10.0	0.5					2	1286	511	1005	
10.5	0.5					4	1456	604	1295	
11.0	0.5					6	1795	465	1669	
11.5	0.5					2	2146	498	2150	
12.0	0.5					0			2770	
12.5	0.5					2	3033	965	3569	
13.0	0.5					4	9054	8953	4599	
13.5	0.5					0			5925	
14.0	0.5					1	8323		7635	

Table 4.  $V=0$  Apparent Angular Size  $q_{V=0}$  as a function of V-K color bin. The number of stars  $N$ , average size  $q_{V=0}$ , and standard deviation for each bin is given for both normal giant and supergiant stars, and for variables, inclusive of Miras, semi-regulars, and carbon stars.

significantly with spatial proximity. {quantification of this phenomenon in Boden *et al.* 1998 iota Peg paper?} Similar evidence exists for the IOTA interferometer, although it is not as well quantified (Dyck *et al.* 1996); nevertheless, our selection of calibration sources for IOTA employed identical restrictions. For the Mark III interferometer, the proximity considerations were not as significant, although the users of that particular instrument clearly took care in quantifying that particular aspect of the instrument (Mozurkewich *et al.* 1991).

Clearly it is prudent to understand the response of one's instrument with regards to these considerations.

Specific investigation of the correlation of system response between point-like calibration sources in a variety of circumstances is necessary to give a measure of confidence to results from interferometric instruments, particularly the error bars. Although the necessity of such quantification should be obvious, the use of merely anecdotal evidence in this regard can lead researchers to erroneous conclusions.

## 5. Conclusion

Clearly the use of expected angular sizes to calibrate interferometric data is a task that must be

Method	1 sigma	2 sigma	3 sigma	Notes
Linear Radius by Spectral Type				
Main Sequence Stars	25	42	60	
Giant Stars	22	37	52	
Linear Radius by V-K Color				
Giant Stars	22	36	51	
Angular Size by BBR Fit				
Main Sequence Stars	13	35	57	*
Giant, Supergiant Stars	18	35	52	
FG	8	16	23	*
K	10	17	25	*
M	21	45	69	
V=0 Angular Size by V-K Color				
Main Sequence Stars	2	4	6	*, Limited V-K range
Giant, Supergiant Stars	10	17	25	*
Variable Stars	21	38	54	

Table 5. Comparison of the various methods for obtaining angular size. An asterisk '\*' denotes the preferred methods for predicting calibrator angular sizes.

embarked upon with great care. The use of measured sizes to rigorously quantify the accepted methods of the past, and to explore potential new techniques, is a possibility only now available to the community with the large numbers of angular sizes becoming available in the literature. The approach of establishing the apparent  $\theta_{V=0}$  angular size appears to be a powerful tool in predicting the angular sizes of main sequence and giant/supergiant stars, and also appears to be able to provide insight into the fundamental physical differences between giants/supergiants, and more evolved variables.

## 6. References

- Baldwin, J.E. *et al.*, 1996, *A&A*, **306**, L13.  
Beichman, C.A., Chester, T.J., Skrutskie, M., Low, F.J., Gillett, F., 1998, *PASP*, **110**, 480.  
Benson, J.A., Dyck, H.M., Ridgway, S.T., Dixon, D.J., Mason, W.L., Howell, R.R., 1991, *AJ*, **102**, 2091.  
Colavita, M.M. *et al.*, 1998, *Astronomical Interferometry*, R.D. Reasenberg, ed., *Proc. SPIE*, **3350**, 776.  
Colavita, M.M. *et al.*, 1999, (in press).  
Di Benedetto, G.P. & Conti, G., 1983, *ApJ*, **268**, 309.  
Di Benedetto, G.P., 1985, *A&A*, **148**, 169.  
Di Benedetto, G.P., 1993, *A&A*, **270**, 315.  
Di Giacomo, A., Lisi, F., Calamai, G., Richichi, A., 1991, *A&A*, **249**, 397.  
Dyck, H.M., Benson, J.A., van Belle, G.T., Ridgway, S.T., 1996a, *AJ*, **111**, 1705.  
Dyck, H.M., van Belle, G.T., Benson, J.A., 1996b, *AJ*, **112**, 294.  
Dyck, H.M., 1998a, private communication.  
Dyck, H.M., van Belle, G.T., Thompson, R.R., 1998b, *AJ*, **116**, 981.  
Epchtein, N., 1997, in *The Impact of Large Scale Near-infrared Surveys*, ed. F. Garzon, N. Epchtein, A. Omont, W.B. Burton, & P. Persi (Dordrecht: Kluwer).  
Fracassini, M., Pasinetti-Fracassini, L.E., Pastori, L., Pironi, R., 1988, *Bull. D'Inf. Cent. Donnees Stellaires*, **35**, 121.  
Gezari, D.Y., Schmitz, M., Pitts, P.S., Mead, J.M., 1993, *Catalog of Infrared Observations, 3rd Edition*, NASA Reference Publication 1294.  
Gezari, D.Y., Pitts, P.S., Schmitz, M., 1997, *Catalog of Infrared Observations, Edition 4*, unpublished but available online at <http://adc.gsfc.nasa.gov/>.  
Hanbury Brown, R., Davis, J., Lake, R.J.W., Thompson, R.J., 1974, *MNRAS*, **167**, 475.  
Maroitti, J.-M. *et al.* 1998, *Astronomical Interferometry*, R.D. Reasenberg, ed., *Proc. SPIE*, **3350**, 800.  
McAlister, H.A., Bagnuolo, B.G., ten Brummelaar, T., Hartkopf, W. I., Turner, N. H., Garrison, A.K., Robinson, B.G., Ridgway, S.T., 1994, *Amplitude and Intensity Spatial Interferometry II*, James B. Breckinridge, Ed., *Proc. SPIE*, **2200**, 129.  
Mozurkewich, D., Johnston, K. J., Simon, Richard S., Bowers, P. F., Gaume, Ralph, Hutter, D. J., Colavita, M. M., Shao, M., Pan, X. P. 1991, *AJ*, **101**, 2207.  
Perrin, G., Coudé du Foresto, V., Ridgway, S.T., Mariotti, J.-M., Traub, W.A., Carleton, N.P., Lacasse, M.G., 1998, *A&A*, **331**, 619.  
Perryman, M. A. C., Lindegren, L., Kovalevsky, J., Hog, E., Bastian, U., Bernacca, P. L., Creze, M., Donati, F., Grenon, M., Grewing, M., Van Leeuwen, F., Van Der Marel, H., Mignard, F., Murray, C. A., Le Poole, R. S., Schrijver, H., Turon, C., Arenou, F., Froeschle, M., Petersen, C. S., 1997, *A&A*, **323**, L49.  
Richichi, A., Salnari, P., Lisi, F., 1988, *ApJ*, **326**, 791.  
Richichi, A., Lisi, F., Calamai, G., 1991, *A&A*, **241**, 131.  
Richichi, A., Lisi, F., Di Giacomo, A., 1992, *A&A*, **254**, 149.

- Richichi, A., Di Giacomo, A., Lisi, F., Calamai, G., 1992, *A&A*, **265**, 535.
- Richichi, A., Chandrasekhar, T., Lisi, F., Howell, R.R., Meyer, F., Rabbia, Y., Ragland, S., Ashok, N.M., 1995, *A&A*, **301**, 439.
- Richichi, A., Ragland, S., Fabbroni, L., 1998a, *A&A*, **330**, 578.
- Richichi, A., Stecklum, B., Herbst, T.M., Lagage, P.-O., Thamm, E., 1998b, *A&A*, **334**, 585.
- Richichi, A., Ragland, S., Stecklum, B., Leinert, C., 1998c, *A&A*, **338**, 527.
- Richichi, A., *et al.* 1998d, (in preparation).
- Ridgway, S.T., Jacoby, G.H., Joyce, R.R., Wells, D.C., 1980, *AJ*, **85**, 1496.
- Ridgway, S.T., Wells, D.C., Joyce, R.R., 1977, *AJ*, **82**, 414.
- Scholz, M., Takeda, Y., 1987, *A&A*, **186**, 200.
- Tuthill, P.G., 1994, PhD Dissertation, University of Cambridge.
- van Belle, G.T., Dyck, H.M., Benson, J.A., Lacasse, M.G., 1996, *AJ*, **112**, 2147.
- van Belle, G.T., Dyck, H.M., Thompson, R.R., Benson, J.A., Kannappan, S.J., 1997, *AJ*, **114**, 2150.
- van Belle, G.T., *et al.* 1999 *AJ* (in press).

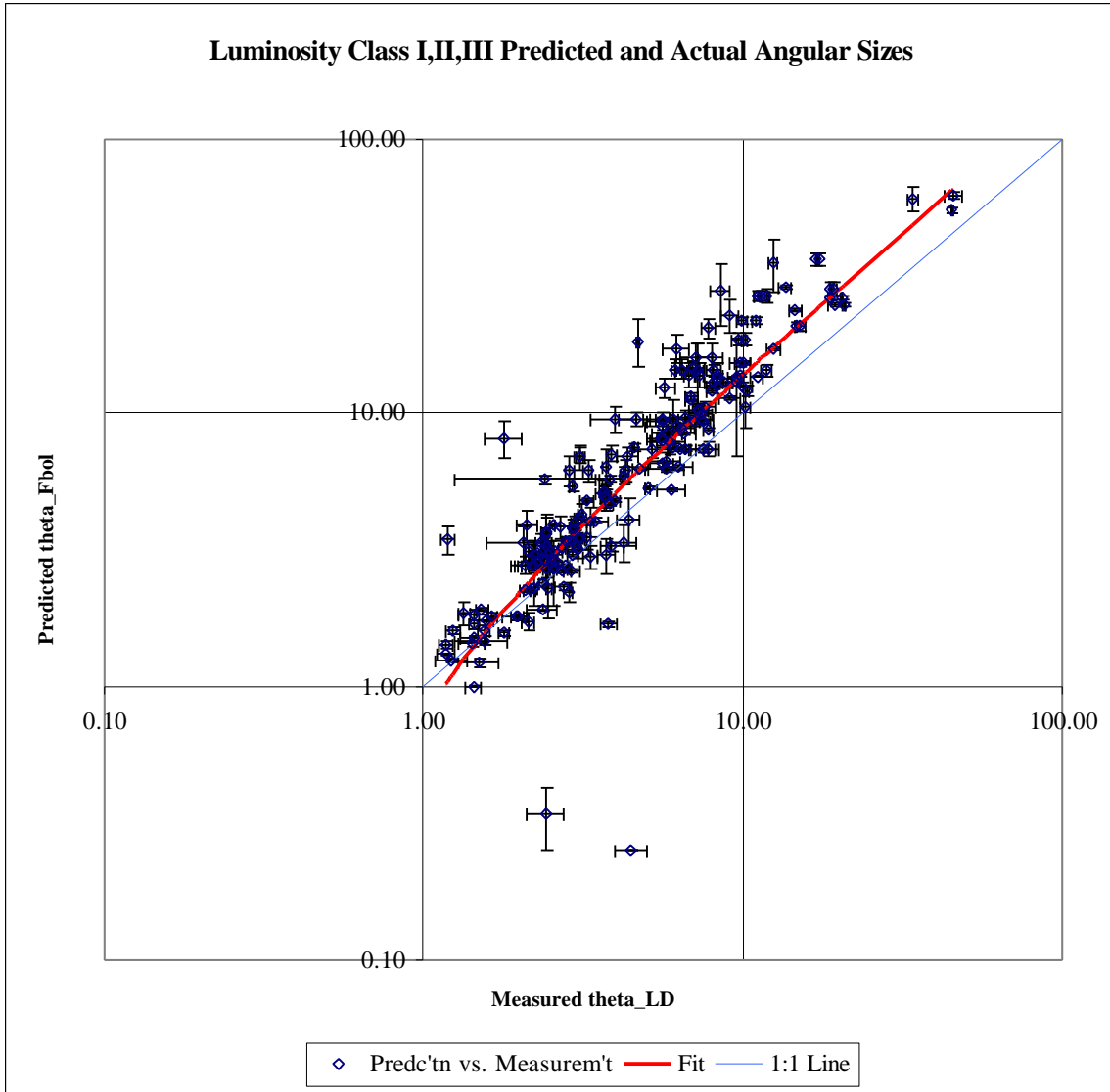


Figure 1. Predicted blackbody radiator (BBR) angular sizes versus measured angular sizes for luminosity class I, II and III objects of all available spectral types. The BBR equals measured angular size diagonal line is also shown for comparison.

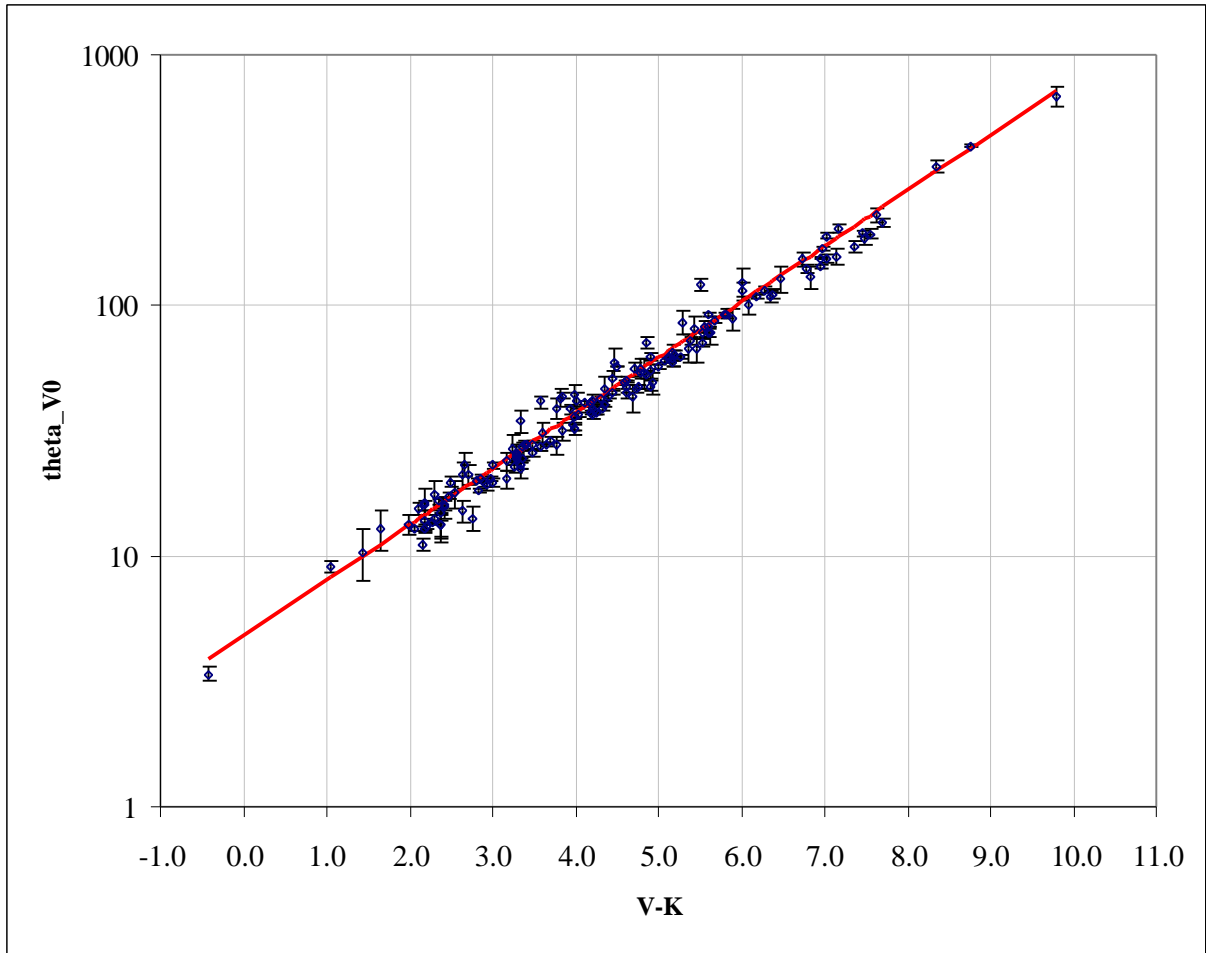


Figure 2. The V=0 apparent angular size versus V-K color for luminosity class III giant stars.

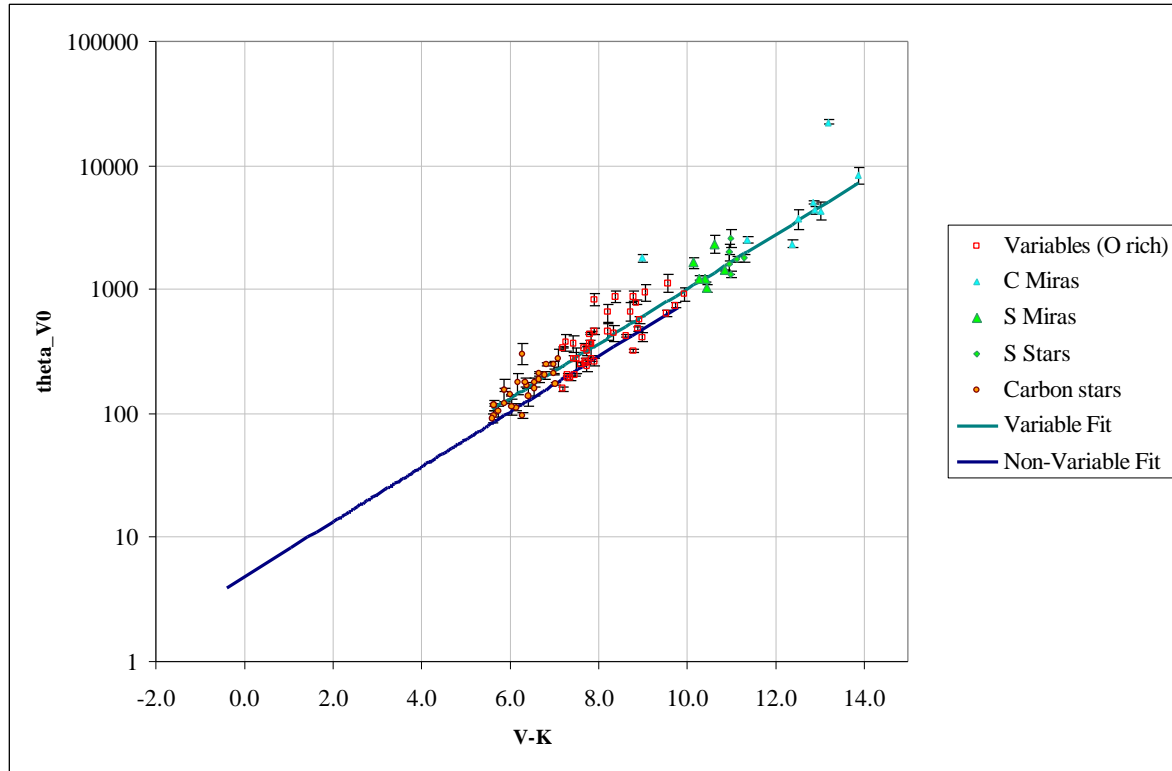


Figure 3. The  $V=0$  apparent angular size versus  $V-K$  color for evolved stars, including Mira variables, S stars, carbon stars, and non-Mira variables. The upper line is the fit line for these objects, the lower line is the fit line for the luminosity class III giants.

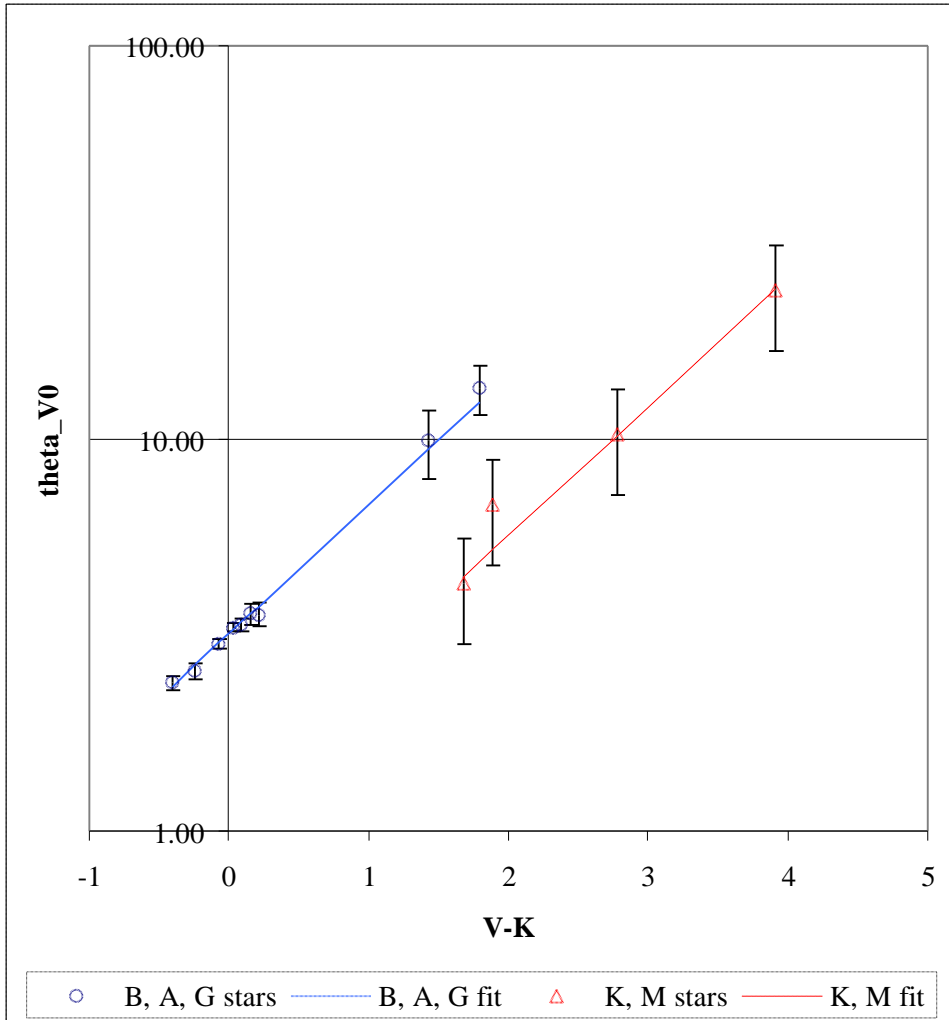


Figure 4. The  $V=0$  apparent angular size versus  $V-K$  color for main sequence stars. The circles and solid line are the data points and fit for B, A, and G type stars, respectively; the triangles and dotted line are the data points and fit for K, M stars, respectively.